

## DYNAMIC ELASTIC AND PLASTIC BUCKLING OF COMPLETE SPHERICAL SHELLS

NORMAN JONES† and CHUNG S. AHN‡

Massachusetts Institute of Technology, Department of Ocean Engineering,  
Cambridge, Massachusetts 02139 U.S.A.

(Received 18 December 1973; revised 11 March 1974)

**Abstract**—A theoretical investigation is undertaken into the dynamic instability of complete spherical shells which are loaded impulsively and made from either linear elastic or elastic-plastic materials. It is shown that certain harmonics grow quickly and cause a shell to exhibit a wrinkled shape which is characterized by a critical mode number. The critical mode numbers are similar for spherical and cylindrical elastic shells having the same  $R/h$  ratios and material parameters, but may be larger or smaller in an elastic-plastic spherical shell depending on the values of the various parameters. Threshold velocities are also determined in order to obtain the smallest velocity that a shell can tolerate without excessive deformation. The threshold velocities for the elastic and elastic-plastic spherical shells are larger than those which have been published previously for cylindrical shells having the same  $R/h$  ratios and material parameters.

### NOTATION

$h$	shell thickness
$t$	time
$E, E_t$	Young's and tangent moduli, respectively
$R$	mean radius of spherical shell
$V_0$	initial impulsive velocity
$\beta^2$	$\frac{2(1-\nu)}{\lambda+1-2\nu}$
$\varepsilon_y, \sigma_e$	equivalent yield strain and equivalent stress, respectively
$\lambda$	$E/E_t$
$\lambda_n$	$n(n+1)$
$\nu, \rho$	Poisson's ratio and density, respectively
$\sigma_y$	yield stress
$(\dot{\phantom{x}})$	$\partial(\phantom{x})/\partial t$ or $\partial(\phantom{x})/\partial \tau$
$(\phantom{x})_{,x}$	$\partial(\phantom{x})/\partial x$ , where $x = \theta, \phi, \tau$ or $y$ .

### INTRODUCTION

A theoretical procedure was developed in [1] in order to examine the dynamic plastic buckling of complete spherical shells which were loaded with an external impulsive velocity and made from a rigid-plastic material. These theoretical predictions are expected to be useful for thin-walled spherical shells with small  $R/h$  ratios (e.g.  $10 < R/h < 60$ ). However, material elasticity exercises an important influence on the dynamic response of spherical shells with large  $R/h$  ratios (e.g.  $R/h > 350$ ). Thus, the dynamic behavior of complete spherical shells which are made from either linear elastic or elastic-plastic materials is investigated herein.

†Associate Professor, Department of Ocean Engineering, Massachusetts Institute of Technology, Cambridge, Massachusetts 02139, U.S.A.

‡Environmental Scientist, Environmental Equipment Division, E. G. & G., Waltham, Massachusetts, U.S.A.

An examination is made of the influence of small deviations from sphericity of the shell and the effect of small perturbations in the initial uniform velocity field. It turns out that certain harmonics grow very quickly and cause a spherical shell to exhibit a characteristic wrinkled shape. It is assumed in the elastic-plastic case that the strains which are associated with the perturbed state are much smaller than those associated with the predominant motion. Thus, no unloading of the shell material occurs before the time when all the initial kinetic energy is absorbed by the spherical shell in the predominant mode. Moreover, it is further assumed that the wrinkled pattern in the shells is established prior to this time and is not modified by subsequent unloading.

#### BASIC EQUATIONS

A set of membrane strain and curvature displacement relations were developed in [2] for arbitrarily shaped thin shells with strains that were small compared to unity and with transverse deflections  $W$  which were much larger than the in-plane displacements  $U$  and  $V$ . The usual thin shell assumption  $h/R \ll 1$  was introduced during the theoretical analysis. However, if this thinness simplification was delayed in the analysis until the final expansions for the strains, then the membrane strain rates for the particular case of a spherical shell are

$$\dot{\epsilon}_\phi = \left( \dot{U}_{,\phi} - \dot{W} + \frac{1}{R} W_{,\phi} \dot{W}_{,\phi} \right) / R \quad (1a)$$

$$\dot{\epsilon}_\theta = (\text{cosec } \phi \dot{V}_{,\theta} + \cot \phi \dot{U} - \dot{W} + \text{cosec}^2 \phi W_{,\theta} \dot{W}_{,\theta} / R) / R \quad (1b)$$

$$\dot{\epsilon}_{\phi\theta} = [\text{cosec } \phi \dot{U}_{,\theta} - \cot \phi \dot{V} + \dot{V}_{,\phi} + \text{cosec } \phi (W_{,\phi} \dot{W}_{,\theta} + W_{,\theta} \dot{W}_{,\phi}) / R] / R \quad (1c)$$

which agree with the predictions of Ref.[2], while the curvature rate expressions are

$$\dot{\kappa}_\phi = (\dot{W} + \dot{W}_{,\phi\phi}) / R^2 \quad (1d)$$

$$\dot{\kappa}_\theta = (\dot{W} + \text{cosec}^2 \phi \dot{W}_{,\theta\theta} + \cot \phi \dot{W}_{,\phi}) / R^2 \quad (1e)$$

and

$$\dot{\kappa}_{\phi\theta} = 2[\text{cosec } \phi \dot{W}_{,\phi\theta} - \cot \phi \text{cosec } \phi \dot{W}_{,\theta}] / R^2 \quad (1f)$$

which are the same as Ref.[2] except for the presence of the  $\dot{W}/R^2$  terms in equations (1d) and (1e) and the absence of any terms containing the in-plane displacements  $U$  and  $V$ . The present approach also leads to non-linear terms in the curvature-displacement expressions but these are not considered herein. The displacements are defined as shown in Fig. 1 and  $(\dot{\phantom{x}}) = \partial(\phantom{x})/\partial t$  where  $t$  is time. The principle of virtual work may be used to obtain the equilibrium equations

$$N_{\phi,\phi} + \cot \phi (N_\phi - N_\theta) + \text{cosec } \phi N_{\phi\theta,\theta} - \rho h R \ddot{U} + P_1 R = 0 \quad (2a)$$

$$\text{cosec } \phi N_{\theta,\theta} + N_{\phi\theta,\phi} + 2 \cot \phi N_{\phi\theta} - \rho h R \ddot{V} + P_2 R = 0 \quad (2b)$$

and

$$\begin{aligned} & R(N_\phi + N_\theta) + N_\phi (W_{,\phi\phi} + \cot \phi W_{,\phi}) + N_\theta \text{cosec}^2 \phi W_{,\theta\theta} \\ & + \text{cosec } \phi N_{\phi\theta} (W_{,\phi\theta} + W_{,\theta\phi}) + (N_{\phi,\phi} W_{,\phi} + W_{,\theta} N_{\phi\theta,\phi} \text{cosec } \phi + \\ & + W_{,\phi} N_{\phi\theta,\theta} \text{cosec } \phi + \text{cosec}^2 \phi N_{\theta,\theta} W_{,\theta}) - (M_{\phi,\phi\phi} + \\ & + 2 \cot \phi M_{\phi,\phi} - \cot \phi M_{\theta,\phi} + 2M_\theta + \text{cosec}^2 \phi M_{\theta,\theta\theta} + \\ & + 2 \text{cosec } \phi M_{\phi\theta,\phi\theta} + 2 \text{cosec } \phi \cot \phi M_{\phi\theta,\theta}) - R^2 \rho h \ddot{W} + R^2 P_3 = 0 \end{aligned} \quad (2c)$$

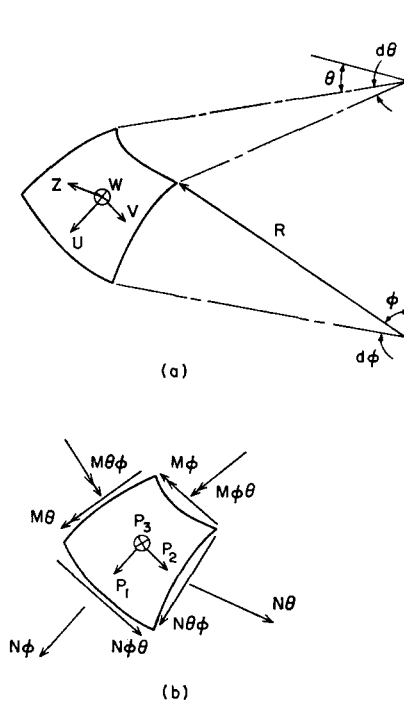


Fig. 1. (a) Displacements and (b) membrane forces, bending moments and external loads on a spherical shell.

which are consistent with the strain and curvature expressions (1a)–(1f) provided the influence of transverse shear deformation is disregarded.

It may be shown by direct substitution that the strain and change of curvature relations given by equations (1a)–(1f) satisfy the compatibility equation

$$\dot{e}_{\theta,\phi\phi} + \operatorname{cosec}^2 \phi \dot{e}_{\phi,\theta\theta} + 2 \cot \phi \dot{e}_{\theta,\phi} - \cot \phi \dot{e}_{\phi,\phi} + 2 \dot{e}_{\phi} - \operatorname{cosec} \phi \dot{e}_{\phi\theta,\phi\theta} - \operatorname{cosec} \phi \cot \phi \dot{e}_{\phi\theta,\theta} + R(\dot{\kappa}_{\phi} + \dot{\kappa}_{\theta}) = 0 \quad (3)$$

for infinitesimal displacements.

Constitutive equations for arbitrarily shaped shells which are made from an elastic-plastic material are developed in Ref. [3] and discussed briefly in the Appendix which accompanies this article. Equations (1.20a)–(1.21c) of Ref. [3] can be written for a spherical shell in the form

$$\dot{N}_{\phi} = \frac{Eh}{\Delta} [C_2 \dot{e}_{\phi} + C_{12} \dot{e}_{\theta}], \quad \dot{N}_{\theta} = \frac{Eh}{\Delta} [C_1 \dot{e}_{\theta} + C_{12} \dot{e}_{\phi}] \quad (4a, b)$$

$$\dot{M}_{\phi\theta} = \frac{Eh}{\Delta} C_3 \dot{e}_{\phi\theta}, \quad \dot{M}_{\phi} = \frac{Eh^3}{12\Delta} [C_2 \dot{\kappa}_{\phi} + C_{12} \dot{\kappa}_{\theta}] \quad (4c, d)$$

$$\dot{M}_{\theta} = \frac{Eh^3}{12\Delta} [C_1 \dot{\kappa}_{\theta} + C_{12} \dot{\kappa}_{\phi}], \quad \dot{M}_{\phi\phi} = \frac{Eh^3}{12\Delta} C_3 \dot{\kappa}_{\phi\phi} \quad (4e, f)$$

where

$$C_1 = C_2 = \lambda + 3, \quad C_{12} = 4\nu - (\lambda - 1) \quad (5a-c)$$

$$C_3 = \lambda + 1 - 2\nu, \quad \lambda = E/E_t, \quad \Delta = 2(1 + \nu)(\lambda + 1 - 2\nu) \quad (5d, f)$$

when it is assumed that  $q = \sigma_\theta / \sigma_\phi = 1$  for a complete spherical shell loaded uniformly.

It is assumed that the displacements in a complete spherical shell consist of dominant ( $\bar{W}, \bar{U} = \bar{V} = 0$ ) and perturbation ( $W', U', V'$ ) parts so that

$$W(\phi, \theta, \tau) = \bar{W}(\tau) + W'(\phi, \theta, \tau) \quad (6a)$$

$$U(\phi, \theta, \tau) = U'(\phi, \theta, \tau) \quad (6b)$$

and

$$V(\phi, \theta, \tau) = V'(\phi, \theta, \tau). \quad (6c)$$

Thus, the dominant strains and curvature changes are

$$\bar{\epsilon}_\phi = \bar{\epsilon}_\theta = -\bar{W}/R, \quad \bar{\epsilon}_{\phi\theta} = 0 \quad (7a-c)$$

and

$$\bar{\kappa}_\phi = \bar{\kappa}_\theta = \bar{W}/R^2, \quad \bar{\kappa}_{\phi\theta} = 0 \quad (8a-c)$$

respectively, while the corresponding perturbation quantities are given by equations (1a)–(1f) with primes. Similarly,

$$N_\phi(\phi, \theta, \tau) = \bar{N}(\tau) + N'_\phi(\phi, \theta, \tau) \quad (9a)$$

$$N_\theta(\phi, \theta, \tau) = \bar{N}(\tau) + N'_\theta(\phi, \theta, \tau) \quad (9b)$$

and

$$N_{\phi\theta}(\phi, \theta, \tau) = N'_{\phi\theta}(\phi, \theta, \tau) \quad (9c)$$

together with equations (9d)–(9f) for the bending moments which are the same as equations (9a)–(9c) except with  $M$  replacing  $N$ . If equations (6) and (9) are substituted into equation (2c) then the dominant and perturbation transverse equilibrium equations are

$$2\bar{N}/R - 2\bar{M}/R^2 + P_3 - \rho h \ddot{\bar{W}} = 0 \quad (10a)$$

and

$$\begin{aligned} R(N'_\phi + N'_\theta) + \bar{N}(W'_{,\phi\phi} + \cot \phi W'_{,\phi} + \operatorname{cosec}^2 \phi W'_{,\theta\theta}) - \\ - [M'_{\phi,\phi\phi} + 2 \cot \phi M'_{\phi,\phi} - \cot \phi M'_{\theta,\phi} + 2M'_\theta + \operatorname{cosec}^2 \phi M'_{\theta,\theta\theta} \\ + 2 \operatorname{cosec} \phi M'_{\phi\theta,\theta\phi} + 2 \operatorname{cosec} \phi \cot \phi M'_{\phi\theta,\theta}] - \rho h R^2 \ddot{W}' = 0 \end{aligned} \quad (10b)$$

respectively, when neglecting higher order quantities.

It may be shown that the in-plane equilibrium equations (2a) and (2b) are satisfied identically when

$$\dot{N}_\phi = \frac{1}{R^2} [F + \operatorname{cosec}^2 \phi F_{,\theta\theta} + \cot \phi F_{,\phi}], \quad \dot{N}_\theta = \frac{1}{R^2} [F + F_{,\phi\phi}] \quad (11a, b)$$

and

$$\dot{N}_{\phi\theta} = -\frac{1}{R^2} \operatorname{cosec} \phi [F_{,\phi\theta} - \cot \phi F_{,\theta}] \tag{11c}$$

where  $F$  is a stress rate function and  $U = V = P_1 = P_2 = 0$ . Now, substituting equations (4a)–(4c) and (11a)–(11c) into the compatibility equation (3) gives

$$4(1 - \nu)(\nabla^2 + 2)u_{,\tau} + [C_1(\nabla^2 + 1) - C_{12}](\nabla^2 + 2)\tilde{F} = 0 \tag{12a}$$

where

$$u = \frac{W'}{R}, \quad \tilde{F} = \frac{F(1 - \nu)}{EhRC}, \quad C^2 = \frac{E}{\rho(1 - \nu)}, \quad \tau = \frac{C}{R} t \tag{12b-e}$$

$$\nabla^2(\ ) = (\ )_{,\phi\phi} + \cot \phi (\ )_{,\phi} + \operatorname{cosec}^2 \phi (\ )_{,\theta\theta}. \tag{12f}$$

If equations (1, 4, 7–9 and 11) are substituted into equations (10a) and (10b), then the transverse equilibrium equations (10a) and (10b) can be written in the non-dimensionalized form

$$-u_{0,\tau\tau} + 2(1 + \alpha^2) \int^\tau \tilde{\sigma}_{,\tau} d\tau + \tilde{P} = 0 \tag{13a}$$

and

$$u_{,\tau\tau\tau} - (\nabla^2 + 2)\tilde{F} - [\tilde{\sigma}(\tau)\nabla^2 u]_{,\tau} + \alpha^2 \beta^2 a_0 \left[ (\nabla^2 + 1) + \frac{C_{12}}{C_1} \right] (\nabla^2 + 2)u_{,\tau} = 0 \tag{13b}$$

where

$$u_0 = \frac{\bar{W}}{R}, \quad \tilde{\sigma} = \frac{\bar{N}(1 - \nu)}{Eh}, \quad \tilde{P} = \frac{P_3 R(1 - \nu)}{Eh}, \quad \alpha^2 = \frac{1}{12} \left( \frac{h}{R} \right)^2 \tag{14a-d}$$

$$\beta^2 = \frac{2(1 - \nu)}{\lambda + 1 - 2\nu}, \quad \text{and} \quad a_0 = \frac{C_1}{C_1 + C_{12}}. \tag{14e, f}$$

### STATIC BUCKLING

Equation (13a) for the static case predicts

$$\tilde{\sigma} = -\tilde{P}/2 \tag{15}$$

when  $\alpha^2 \ll 1$ . If  $u$  and  $\tilde{F}$  are written in the series expansions

$$u = a_{on} P_n(\cos \phi) + P_n^m(\cos \phi)(a_{mn} \cos m\theta + b_{mn} \sin m\theta) \tag{16a}^\dagger$$

and

$$\tilde{F} = c_{on} P_n(\cos \phi) + P_n^m(\cos \phi)(c_{mn} \cos m\theta + d_{mn} \sin m\theta) \tag{16b}^\dagger$$

where

$$\lambda_n = n(n + 1) \tag{16c}$$

and  $P_n$  and  $P_n^m$  are Legendre and associated Legendre polynomials of degree  $n$  and order  $m$ , then equations (12a) and (13b) give

$$[C_1(\lambda_n - 1) + C_{12}](\lambda_n - 2)c_{mn} - 4(1 - \nu)(\lambda_n - 2)a_{mn,\tau} = 0 \tag{17a}$$

† The summation convention is used for the integers  $m$  and  $n$  with  $0 \leq n \leq \infty$  and  $1 \leq m \leq n$ .

and

$$(\lambda_n - 2)c_{mn} + (\tilde{\sigma}\lambda_n a_{mn})_{,\tau} + \alpha^2 \beta^2 a_0 \left[ \left( \lambda_n - 1 - \frac{C_{12}}{C_1} \right) (\lambda_n - 2) \right] a_{mn,\tau} = 0 \quad (17b)$$

respectively. Two additional equations are also obtained but these are identical to equations (17a) and (17b) provided  $b_{mn}$  and  $d_{mn}$  are substituted for  $a_{mn}$  and  $c_{mn}$ . If  $c_{mn}$  is eliminated from equations (17a) and (17b) then

$$[(\tilde{\omega}_s + \tilde{\sigma}\lambda_n)a_{mn}]_{,\tau} = 0 \quad (18a)$$

where

$$\tilde{\omega}_s = \frac{4(1-\nu)(\lambda_n - 2)}{C_1(\lambda_n - 1) + C_{12}} + \alpha^2 \beta^2 a_0 \left[ \left( \lambda_n - 1 - \frac{C_{12}}{C_1} \right) (\lambda_n - 2) \right]. \quad (18b)$$

Now, when substituting equation (15) into (18a) and integrating it may be shown that static buckling occurs if  $\tilde{P} = 2\tilde{\omega}_s/\lambda_n$  and attains a minimum value when  $\lambda_n \approx \frac{2}{\alpha\beta} \left\{ \frac{(1-\nu)}{C_1 a_0} \right\}^{1/2}$  provided  $\lambda_n \gg 1$ . Thus,  $\lambda_n = 2[3(1-\nu^2)]^{1/2} R/h$  for the linear elastic case ( $\lambda = 1$ ) which agrees with the theoretical predictions of Koiter [4] and with Ref.[5] when  $R/h \gg 1$ . The buckling pressure for an elastic-plastic spherical shell is therefore

$$P \approx 4E \left( \frac{h}{R} \right)^2 \frac{1}{\sqrt{6(\lambda + 1 - 2\nu)(1 + \nu)}} \quad (19)$$

which agrees with the theoretical predictions of Bijlaard[6], Batterman[7] and Hutchinson[8] and with Refs.[4, 5] for the linear elastic case ( $\lambda = 1$ ).

#### DYNAMIC BUCKLING

The solution of the predominant transverse equation of motion (13a) during the initial elastic response of a spherical shell is

$$u_0 = \frac{V_0}{C\sqrt{2}} \sin \sqrt{2}\tau, \quad \text{and} \quad \tilde{\sigma} = -u_0 \quad (20a, b)$$

provided  $\tau \leq \tau_0$ , where  $\tau_0$  is the non-dimensional time when yielding occurs for sufficiently large values of the uniformly distributed external impulsive velocity  $V_0$ . It is evident from equation (20a) that the predominant response would remain elastic when

$$\frac{2V_0}{\sqrt{2}C} \leq \varepsilon_y \quad \text{or} \quad \rho \frac{V_0^2}{\sigma_y} \leq \frac{\varepsilon_y}{2(1-\nu)} \quad (21)$$

where  $\varepsilon_y$  is the equivalent yield strain. If  $\tau \geq \tau_0$  then equation (13a) has the solution

$$u_0 = D \sin[\sqrt{2}\beta(\tau - \tau_0) + \psi] - \left( \frac{1 - \beta^2}{\beta^2} \right) \varepsilon_y \quad (22a)$$

where

$$D = \frac{1}{\beta} \left[ \frac{1}{2} \left( \frac{V_0}{C} \right)^2 + \frac{1 - \beta^2}{\beta^2} e_y^2 \right]^{1/2}, \quad \psi = \tan^{-1} \left( \frac{1}{\beta} \tan \sqrt{2} \tau_0 \right) \tag{22b, c}$$

$$e_y = \frac{V_0}{C\sqrt{2}} \sin \sqrt{2} \tau_0, \quad \text{and} \quad \tilde{\sigma} = -\beta^2 D \sin[\sqrt{2}\beta(\tau - \tau_0) + \psi] \tag{22d, e}$$

since  $u_0$ ,  $u_{0,\tau}$  and  $u_{0,\tau\tau}$  are continuous at  $\tau = \tau_0$  between the elastic and plastic stages and provided  $\beta$  (i.e.  $\lambda$ ) is time-independent. The motion of a shell is described by equation (22a) until unloading commences at  $\tau_f$  where

$$\tau_f = \tau_0 + \frac{\pi/2 - \psi}{\sqrt{2}\beta} \tag{23}$$

is given by the condition  $\dot{u}_0 = 0$ . In order to avoid a study of unloading in the perturbation analysis to be considered next, it is assumed when the inequality (21) is violated that the final pattern of wrinkling is established in a spherical shell before  $\tau_f$  when strain reversal occurs.

Now, the solutions for  $u$  and  $\tilde{F}$  are expressed in the form of the infinite series expansions (16a) and (16b). If equations (16a) and (16b) are substituted into the governing equations (12a) and (13b), then a procedure similar to that employed to derive equation (18a) for the static case gives

$$a_{mn,yyy} + g^2 \Lambda^2 (\Lambda^2 - \sin y) a_{mn,y} - g^2 \Lambda^2 \cos y a_{mn} = 0 \tag{24a} \ddagger$$

when assuming  $\tilde{\sigma}$  is given by equation (22e) and where

$$y = \sqrt{2}\beta(\tau - \tau_0) + \psi, \quad g^2 \Lambda^2 = \frac{D\lambda_n}{2}, \quad \text{and} \quad \Lambda^2 = \frac{\tilde{\omega}_s}{\lambda_n \beta^2 D}. \tag{24b-d}$$

Another equation is also obtained which is similar to equation (24a) but with  $b_{mn}$  substituted for  $a_{mn}$ .

A series solution for the time dependence of  $a_{mn}$  which satisfies equation (24a) is now sought. The general procedure which follows is similar to that developed by Stuiver [9] for the dynamic plastic buckling of rings and is suggested by the series expansions used by Whittaker and Watson [10] to obtain the solution of a Mathieu–Hill equation.‡ If

$$z = \frac{y}{2} + \frac{\pi}{4} \quad \text{and} \quad x = 2g\Lambda^2 \tag{25a, b}$$

then equation (24a) can be rewritten

† If the consistent set of strain and curvature relations and equilibrium equations which are developed in Ref. [2] are used instead of equations (1) and (2), then equation (24a) is again obtained provided only those terms involving transverse displacements ( $W$ ) are retained in the curvature relations and the  $(\lambda_n - 1 - C_{12}/C_1)(\lambda_n - 2)$  term in  $\tilde{\omega}_s$ , (equation 18b) is replaced by  $(\lambda_n - 1 + C_{12}/C_1)\lambda_n$ . Thus, the theoretical predictions according to these two sets of basic equations give identical predictions when  $\lambda_n \gg 1$ .

‡ If equations (25a) and (25b) are substituted into equation (24a), then equation (24a) is recognized as a Mathieu equation differentiated with respect to  $z$ .

$$\phi_{,zzz} \pm 3\omega\phi_{,zz} + \left[ 3\omega^2 + x^2 \left( 1 + \frac{2g}{x} \cos 2z \right) \right] \phi, z + \left[ \pm\omega^3 \pm x^2\omega \left( 1 + \frac{2g}{x} \cos 2z \right) - 4gx \sin 2z \right] \phi = 0 \quad (26a)$$

when it is assumed that

$$a_{mn} = \sum_{k=-\infty}^{\infty} (A_1 e^{\omega z} + A_2 e^{-\omega z}) b_k e^{i2kz} \quad (26b)^\dagger$$

and

$$\phi = \sum_{k=-\infty}^{\infty} b_k e^{i2kz} \quad (26c)$$

In order to simplify the solution only the real part of equation (26c) with  $k = -1, 0$  and  $1$  is retained in the subsequent analysis. Thus, equation (26a) becomes

$$8d_1 \sin 2z \mp 12\omega d_1 \cos 2z - 2d_1 \left\{ 3\omega^2 + x^2 \left( 1 + \frac{2g}{x} \cos 2z \right) \right\} \sin 2z \pm \left\{ \omega^3 + \omega x^2 \left( 1 + \frac{2g}{x} \cos 2z \right) - 4gx \sin 2z \right\} (b_0 + d_1 \cos 2z) = 0 \quad (27)$$

where  $d_1 = b_1 + b_{-1}$ . The two coupled equations

$$b_0(\omega^2 + x^2) + d_1 xg = 0 \quad \text{and} \quad b_0 2gx + d_1(\omega^2 + x^2 - 12) = 0 \quad (28a, b)$$

immediately follow from equation (27) when employing Galerkin's averaging conditions.‡ A solution to these equations exists if

$$\omega^2 = 6 - x^2 \pm \sqrt{36 + 2g^2 x^2} \quad (29)$$

which has a maximum value with respect to  $\lambda_n$  when

$$\lambda_n = \frac{1}{\sqrt{2D}} \left( \frac{D^4}{4\alpha^4 a_0^2} - 36 \right)^{1/2} \quad (30)$$

provided  $\lambda_n \gg 1$ . The mode factor  $\Lambda$  which is predicted by equations (24d) and (30) is associated with the fastest growing mode (equation 26b). The preferred mode number according to equation (16c) is

$$n = \frac{1}{\sqrt{D}} \left( \frac{D^4}{8\alpha^4 a_0^2} - 18 \right)^{1/4} \quad (31)$$

when using equation (30) and  $\lambda_n \gg 1$ .

The approximate solution of equation (24a) can now be written with the aid of equations (25a, 25b, 26b, 26c, 28a and 29)

$$a_{mn} = \left\{ B_1 \exp \left[ \omega \left( \frac{y}{2} + \frac{\pi}{4} \right) \right] + B_2 \exp \left[ -\omega \left( \frac{y}{2} + \frac{\pi}{4} \right) \right] \right\} (1 + \delta \sin y) \quad (32a)$$

† In order to simplify the notation, the subscripts  $mn$  are omitted from  $\omega, A_1, A_2$  and  $b_k$ .

‡ Equation (28a) is obtained by integrating equation (27) with respect to  $z$  when  $z_1 \leq z \leq z_1 + \pi$ . Equation (28b) is similarly obtained, but equation (27) is first multiplied by  $\cos 2z$ .



where

$$\delta = \frac{(9 + 2g^4\Lambda^4)^{1/2}}{g^2\Lambda^2} + \frac{3}{g^2\Lambda^2}. \tag{32b}$$

The response is elastic when  $0 \leq \tau \leq \tau_0$ , so that  $y = \sqrt{2}\tau$  and equation (32a) becomes

$$a_{mn} = u_{mn}^i E_{mn}^e + V_{mn}^i F_{mn}^e \tag{33a}$$

where

$$E_{mn}^e = \left( \cosh \omega_e \frac{\tau}{\sqrt{2}} - 2 \frac{\delta_e}{\omega_e} \sinh \omega_e \frac{\tau}{\sqrt{2}} \right) (1 + \delta_e \sin \sqrt{2}\tau) \tag{33b}$$

and

$$F_{mn}^e = \frac{\sqrt{2}}{\omega_e} \left( \sinh \omega_e \frac{\tau}{\sqrt{2}} \right) (1 + \delta_e \sin \sqrt{2}\tau) \tag{33c}$$

are the amplification functions of the initial displacement imperfections ( $u_{mn}^i$ ) and the initial velocity imperfections ( $V_{mn}^i$ ), respectively, and

$$\omega_e^2 = 6 + \left( 36 + \frac{V_0^2 \lambda_n^2}{C^2} \right)^{1/2} - \frac{2}{1 + \nu} \left\{ \frac{(1 - \nu^2)(\lambda_n - 2)}{\lambda_n - 1 + \nu} + \alpha^2(\lambda_n - 1 - \nu)(\lambda_n - 2) \right\} \tag{33d}$$

and

$$\delta_e = \frac{\sqrt{2}C}{V_0 \lambda_n} \left\{ 6 + \left( 36 + \frac{V_0^2 \lambda_n^2}{C^2} \right)^{1/2} \right\} \tag{33e}$$

It should be noted that the initial displacement and velocity imperfections are assumed to be distributed in the infinite series form of equation (16a). Equation (31) predicts the preferred mode number

$$n_e = \left( \frac{C}{V_0} \right)^{1/2} \left\{ 9(1 + \nu)^2 \left( \frac{R}{h} \right)^4 \left( \frac{V_0}{C} \right)^4 - 36 \right\}^{1/4} \tag{34a}$$

which for thin shells can be written

$$n_e \simeq \sqrt{3(1 + \nu)} \left( \frac{R}{h} \right) \left( \frac{V_0}{C} \right)^{1/2} \tag{34b}$$

when

$$n \gg 1 \text{ and } \frac{(1 + \nu)^2}{4} \left( \frac{R}{h} \right)^4 \left( \frac{V_0}{C} \right)^4 \gg 1. \tag{34c}$$

A spherical shell commences to respond plastically at the time  $\tau = \tau_0$  provided the perturbation terms during the elastic stage are negligible compared with the dominant behavior. In this circumstance, equation (32a) becomes

$$a_{mn} = u_{mn}^i E_{mn}^p + V_{mn}^i F_{mn}^p \tag{35a}$$

where

$$E_{mn}^p = E'_{mn} E_{mn}^e(\tau_0) + F'_{mn} E_{mn,\tau}^e(\tau_0) \quad (35b)$$

$$F_{mn}^p = E'_{mn} F_{mn}^e(\tau_0) + F'_{mn} F_{mn,\tau}^e(\tau_0) \quad (35c)$$

$$E'_{mn} = \left[ \frac{1 + \delta_p \sin\{\sqrt{2}\beta(\tau - \tau_0) + \psi\}}{(1 + \delta_p \sin \psi)^2} \right] \cdot \left[ (1 + \delta_p \sin \psi) \cosh\left\{\frac{\omega_p \beta}{\sqrt{2}}(\tau - \tau_0)\right\} - 2 \frac{\delta_p}{\omega_p} \cos \psi \sinh\left\{\frac{\omega_p \beta}{\sqrt{2}}(\tau - \tau_0)\right\} \right] \quad (35d)^\dagger$$

and

$$F'_{mn} = \frac{\sqrt{2}[1 + \delta_p \sin(\sqrt{2}\beta(\tau - \tau_0) + \psi)]}{\omega_p \beta (1 + \delta_p \sin \psi)} \sinh\left\{\omega_p \frac{\beta}{\sqrt{2}}(\tau - \tau_0)\right\} \quad (35e)$$

and where  $E_{mn}^e(\tau_0)$ ,  $E_{mn,\tau}^e(\tau_0)$ ,  $F_{mn}^e(\tau_0)$  and  $F_{mn,\tau}^e(\tau_0)$  are evaluated from equations (33b) and (33c) when  $\tau = \tau_0$ . The coefficients in equation (35a) were selected to ensure that the elastic and plastic solutions matched at  $\tau = \tau_0$ .

Substituting equations (14d, 14f and 22b) into equation (30) gives

$$\lambda_n^p = \frac{3\sqrt{2}\beta}{\left\{\frac{1}{2}\left(\frac{V_0}{C}\right)^2 + \frac{1 - \beta^2}{\beta^2} e_y^2\right\}^{1/2}} \left\{\frac{16}{\beta^4} \left(\frac{1 + \nu}{\lambda + 3}\right)^2 \left(\frac{R}{h}\right)^4 \left[\frac{1}{2}\left(\frac{V_0}{C}\right)^2 + \frac{1 - \beta^2}{\beta^2} e_y^2\right]^2 - 1\right\}^{1/2} \quad (36a)$$

which may be simplified considerably if the amount of material strain hardening is small (i.e.  $\beta^2 \ll 1$  or  $\lambda \gg 1$ ). In this case, equations (16c) and (36a) predict a preferred mode number

$$n_p \approx \left(\frac{3(1 + \nu)\sqrt{2}e_y}{1 - \nu}\right)^{1/2} \left(\frac{R}{h}\right) \left\{2\left(\frac{\beta V_0}{\varepsilon_y C}\right)^2 + 1\right\}^{1/4} \quad (36b)^\ddagger$$

provided

$$\frac{(1 + \nu)\lambda e_y^2}{4(1 - \nu)^2} \left\{2\left(\frac{\beta V_0}{\varepsilon_y C}\right)^2 + 1\right\} \left(\frac{R}{h}\right)^2 \gg 1 \quad (36c)$$

and where  $\varepsilon_y = 2e_y$  is the equivalent yield strain.

It is of interest to determine a critical or threshold impulse which gives a large amplification of the perturbation displacement for a small increment of impulse. If  $\lambda_n \gg 1$ , then equations (24c, 24d, 25b, 29 and 30) give

$$\omega_{crit}^2 = 6 - \frac{8(1 - \nu)}{C_1 \beta^2} + \frac{D^2}{4\alpha^2 a_0} + \frac{36\alpha^2 a_0}{D^2}. \quad (37)$$

The minimum value of equation (37) with respect to  $(V_0/C)^2$  for an elastic shell is  $\omega_{crit}^2 = 10 + 2\nu$  which occurs when

$$\left(\frac{V_0}{C}\right)^2 = \frac{2}{1 + \nu} \left(\frac{h}{R}\right)^2. \quad (38)$$

$^\dagger \delta_p$  and  $\omega_p$  are respectively equations (32b) and (29) evaluated in the plastic region.

$^\ddagger$  The numerical coefficient in equation (36b) is taken as  $2\sqrt{2}$  when  $\nu = 0.3$ .

It is evident from equations (23, 24b, and 25a) when  $\omega = \pi$  that the exponential term in equation (26b) increases rather rapidly with time before unloading commences.

However, in order for the theoretical method to predict the phenomenon of dynamic instability, it is necessary for the amplification function  $E_{mn}^e$  (and/or  $F_{mn}^e$ ) which is associated with the critical harmonic ( $n_c$ ), to be larger than unity. Now, the maximum value of the predominant radial displacement in the elastic case occurs when  $\tau_f = \frac{\pi}{2\sqrt{2}}$  according to equation (20a). At  $\tau = \tau_f$  and  $\omega_e = \omega_{crit}$ , it is evident that  $F_{mn}^e$  given by equation (33c) is positive, while  $E_{mn}^e$  according to equation (33b) is positive if

$$\frac{\rho V_0^2}{\sigma_y} > \frac{6.95}{\epsilon_y} \left(\frac{h}{R}\right)^2 \tag{39}$$

when  $\nu = 0.3$  [3], which is more restrictive than equations (34c) and (38). Thus, equation (39) is used to define a critical velocity or threshold impulse for the elastic case since the associated value of  $\omega_{crit}$  is sufficient to produce a moderate amplification of the initial displacements. The actual values of the amplification functions  $E_{mn}^e$  and  $F_{mn}^e$  can be calculated using equations (33b) and (33c) for a particular shell. The growth of  $E_{mn}^e$  and  $F_{mn}^e$  with time according to equations (33b) and (33c) is indicated in Fig. 2 for an elastic shell with  $R/h = 500$ ,  $V_0/C = 0.015$  and  $\nu = 0.3$ , while the variation of the largest amplification functions at  $\tau = \tau_f$  with  $V_0/C$  for the same shell are indicated in Fig. 3 together with the predictions of (39).

Equation (37) for an elastic-plastic shell with  $\beta^2 \ll 1$  (i.e.  $\lambda \gg 1$ ) has the minimum value  $\omega_{crit} = 2\sqrt{2}$  when [3]

$$\frac{\rho V_0^2}{\sigma_y} = \frac{1}{(1 + \nu)\epsilon_y} \left(\frac{h}{R}\right)^2 - \frac{\lambda\epsilon_y}{4(1 - \nu)^2}. \tag{40a}$$

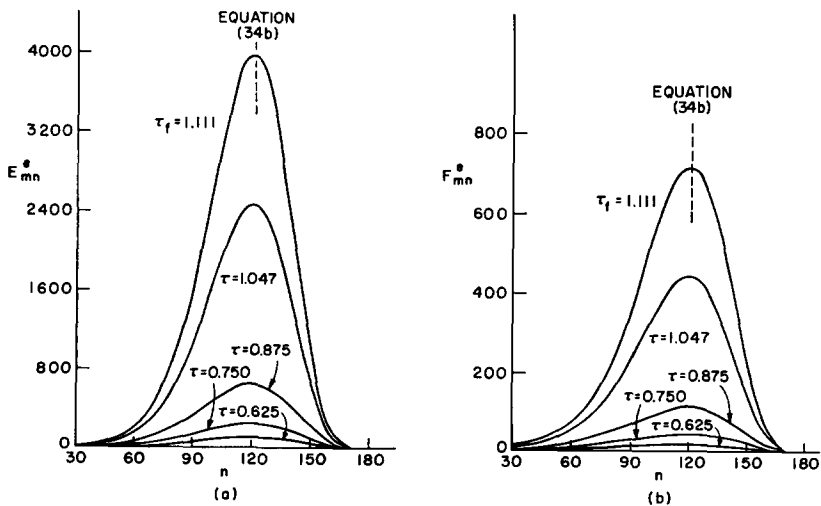


Fig. 2. Growth of amplification functions for an elastic spherical shell with  $R/h = 500$ ,  $V_0/C = 0.015$  and  $\nu = 0.3$ .

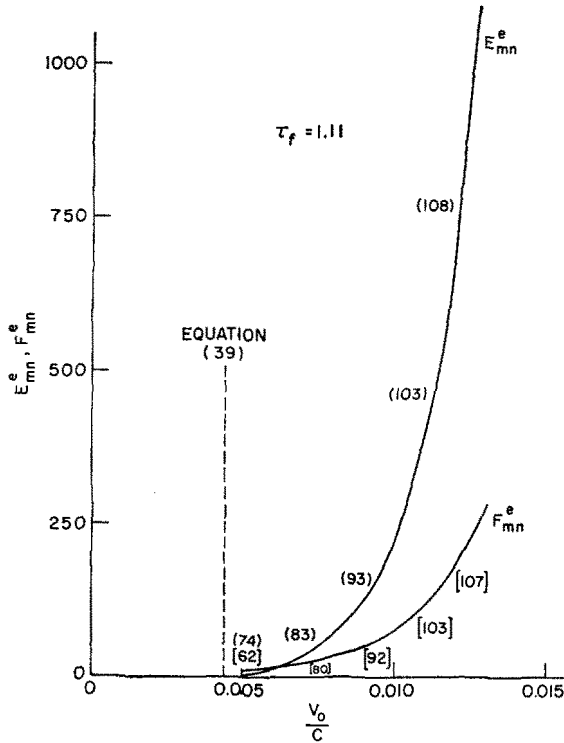


Fig. 3. Variation of largest amplification functions at  $\tau = \tau_f$  with initial impulsive velocity for an elastic spherical shell with  $R/h = 500$  and  $\nu = 0.3$ . The numbers within the parentheses ( ) and [ ] are the critical modes for  $E_{mn}^e$  and  $F_{mn}^e$ , respectively.

If the initial kinetic energy is equated to the predominant membrane energy, then [3]

$$\epsilon_y \approx \rho \beta^2 V_0^2 (1 - \nu) / (2\sigma_y) \tag{40b}$$

provided the final strain which is predicted by equation (22a) with  $\tau = \tau_f$  is much larger than the yield strain ( $\epsilon_y$ ), or

$$\frac{\rho V_0^2}{\sigma_y} > \frac{\epsilon_y}{1 - \nu} \tag{40c}$$

Thus,  $\epsilon_y$  can be eliminated from equation (40a) to give the more convenient form[3]

$$\frac{\rho V_0^2}{\sigma_y} = \frac{2}{1 - \nu} \left\{ \frac{\lambda}{5(1 + \nu)} \right\}^{1/2} \left( \frac{h}{R} \right) \tag{40d}$$

The values of the amplification functions  $E_{mn}^p$  and  $F_{mn}^p$  can be calculated from equations (35b) and (35c) for a particular elastic-plastic shell. The variation of  $E_{mn}^p$  and  $F_{mn}^p$  at  $\tau = \tau_f$  with  $V_0/C$  is shown in Fig. 4 for a given set of parameters, while the variation of  $E_{mn}^p$  and  $F_{mn}^p$  with time is shown in Fig. 5 for the same shell. Again, dynamic buckling could be said to occur in an elastic-plastic shell when the magnitudes of the amplification functions  $E_{mn}^p$  and  $F_{mn}^p$  which are associated with the critical harmonic are much larger than unity. Now the predominant motion reaches its maximum excursion at  $\tau_f$  which is given by equation (23).

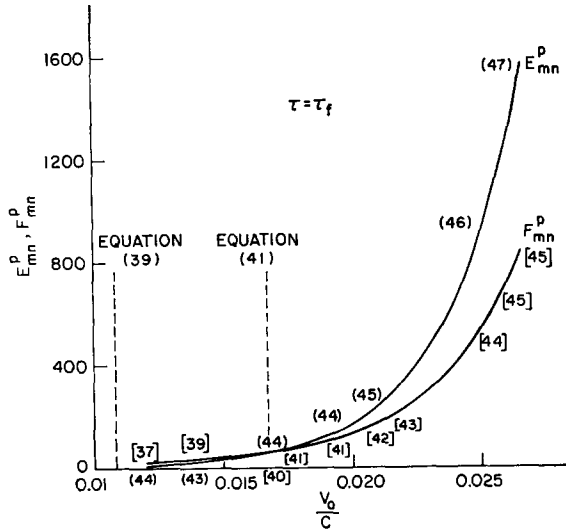


Fig. 4. Variation of largest amplification functions at  $\tau = \tau_f$  with initial impulsive velocity for an elastic-plastic spherical shell with  $R/h = 200$ ,  $\beta_1 = 2.95$ ,  $\nu = 0.33$ ,  $\lambda = 80.8$  and  $e_y = 0.0021$ . The numbers within the parentheses ( ) and [ ] are the critical modes for  $E_{mn}^P$  and  $F_{mn}^P$ , respectively.

Thus, at  $\tau = \tau_f$ ,  $F_{mn}^P$  is always positive, while  $E_{mn}^e(\tau_0) > 0$  provided (39) is satisfied. It can be shown that  $E_{mn}^e > 0$  when  $\omega_p/(2\delta p) > 1$ , or

$$\left(\frac{V_0}{C}\right)^2 > 3.7 \left(\frac{1-\nu}{1+\nu}\right) \left(\frac{h}{R}\right)^2 - \frac{\lambda e_y^2}{1-\nu} \tag{40e}$$

which is a more restrictive requirement than (40a).  $E_{mn}^e(\tau_0) > 0$  when  $2\delta_e/\omega_e < \tanh(\omega_e \tau_0/\sqrt{2})$  which, unfortunately, cannot be recast into a simpler form. Nevertheless, it is

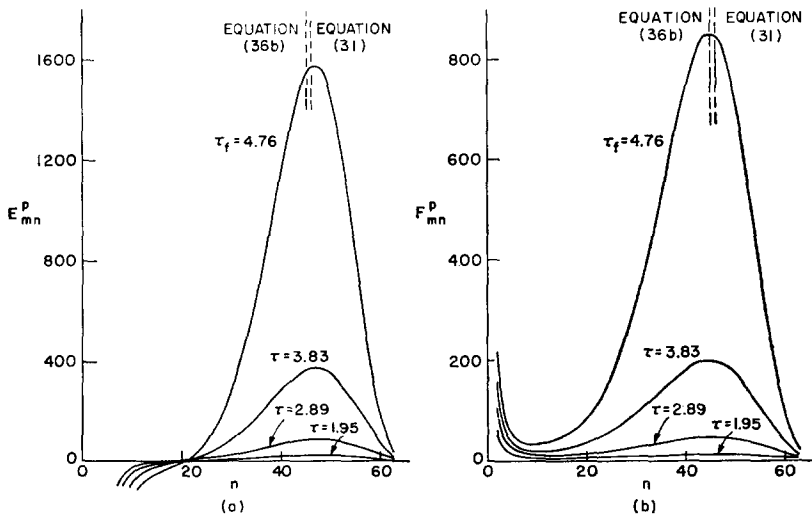


Fig. 5. Growth of amplification functions for an elastic-plastic spherical shell with  $R/h = 200$ ,  $V_0/C = 0.0265$ ,  $\beta_1 = 2.95$ ,  $\nu = 0.33$ ,  $\lambda = 80.8$  and  $e_y = 0.0021$ .

clear that it might not be necessary for all the individual quantities on the right hand side of equation (35a) to remain positive. Indeed, it does appear from some numerical results that  $E_{mn}^e(\tau_0) > 0$  is too restrictive. It is suggested, therefore, that the critical or threshold velocity is the largest of the two values which are predicted by (39) and (40e), the latter of which may be rewritten

$$\frac{\rho V_0^2}{\sigma_y} = \frac{1.72}{1-\nu} \left( \frac{\lambda}{1+\nu} \right)^{1/2} \frac{h}{R} \quad (41)$$

when using equation (40b). The predictions of (39) and (41) are indicated in Fig. 4 for a particular elastic-plastic spherical shell.

### DISCUSSION

As mentioned in Ref. [1] it is of interest to compare the results reported herein with previous theoretical and experimental investigations into the behavior of impulsively loaded rings and cylindrical shells since no theoretical or experimental investigations appear to have been published on the dynamic instability of complete spherical shells.

It is observed that equation (34b) for the critical harmonic† in an impulsively loaded linear elastic spherical shell is almost identical to the prediction of Stuiver [9]: the only differences are that Stuiver defines  $C^2 = E/\rho$  and obtains a numerical coefficient of 2. Equation (34b) is the same as Lindberg's result [11] except that the magnitude of the numerical coefficient is  $\sqrt{3.9/6}$  or about 0.8 times as large. Of course,  $n$ , in the present case, refers to the critical or most amplified harmonic in the displacement field of a complete spherical shell which is expressed in terms of Legendre and associated Legendre polynomials (equation 16a), while in Refs. [9, 11] on rings and cylindrical shells, it is associated with trigonometric functions. It is important to remark that equation (34b) gives meaningful results only when the inequality (34c) is satisfied. Equation (34b) then predicts accurately the peaks in the displacement and velocity amplification curves as shown in Fig. 2 for an elastic spherical shell with  $R/h = 500$ . With the exception of the  $\sqrt{\varepsilon_y} = \sqrt{\sigma_y/E}$  term being replaced by  $\sqrt{\sigma_y/E_t}$ , the form of equation (36b) for the critical harmonic in an elastic-plastic spherical shell is similar to Stuiver's predictions [9] for a ring.

The inequalities (21) and (34c) for an elastic shell can be arranged to provide bounds on  $V_0/C$  which in turn require  $R/h > 2/((\sqrt{1+\nu})\varepsilon_y)$ . Thus, equation (34b) can only be used to predict the critical mode numbers of elastic shells with  $R/h > 350$ , approximately, when  $\varepsilon_y = 2\varepsilon_y = 5 \times 10^{-3}$  and  $\nu = 0.3$ . The sign of inequality (21) is reversed if plastic flow is required to occur during the dominant motion of an elastic-plastic shell. If this inequality is combined with inequality (36c) then upper and lower bounds on  $\varepsilon_y^2$  are obtained. A

comparison of these upper and lower bounds demands  $\frac{R}{h} > \frac{\sqrt{2(1-\nu)}}{\sqrt{(1+\nu)\lambda}} \left( \frac{C}{V_0} \right)$  which must be satisfied if equation (36b) is to predict the critical mode number for an elastic-plastic shell. This inequality, as anticipated, is less restrictive than the previous one for the elastic case. For example, it requires  $R/h > 60$ , approximately, when  $\lambda = 9$ ,  $V_0/C = 5 \times 10^{-3}$  and  $\nu = 0.3$ .

A further examination of inequality (21) also reveals the importance of material elasticity

† The critical harmonics which are predicted by the various formulae in this article are always rounded off to the nearest integer.

for thin shells and material plasticity for thicker ones. The equality in (21), which gives the upper limit of elastic response or lower limit of plastic behavior, may be recast into the form

$$\sqrt{2} \frac{V_0}{C} = \varepsilon_y = 2 \frac{\bar{W}_y}{h} \frac{h}{R}, \text{ since } \varepsilon_y = 2e_y \text{ and } e_y = \bar{W}_y/R, \text{ where } \bar{W}_y \text{ is the transverse dominant}$$

deflection at the onset of plastic flow.† Thus,  $\frac{\bar{W}_y}{h} = \frac{\varepsilon_y R}{2h}$  which indicates that the dominant

transverse deflection-to-shell thickness ratio at yield increases as  $R/h$  increases. If  $\varepsilon_y = 5 \times 10^{-3}$ , then  $\bar{W}_y = 0.025h$  when  $R/h = 10$ , and  $\bar{W}_y = 2.50h$  when  $R/h = 1,000$ .

The concept of a threshold or critical impulse has been used by a number of investigators to mark the smallest impulse that a structure can tolerate without excessive deformation. This definition is somewhat arbitrary, particularly for the elastic case, which hinders comparisons between the theoretical predictions of various authors. Moreover, it is evident from Figures 3 and 4 that the displacement amplification function is a highly non-linear function of the impulsive velocity ( $V_0$ ). The threshold velocity according to equation (39) for a linear elastic spherical shell has the same form as Lindberg's for a cylindrical shell [12] but is

$\left\{ \frac{6.33}{4(1+\nu)} \right\}^{1/2}$  times larger. It can be shown that equation (41) predicts a larger critical velocity for an elastic-plastic spherical shell than Lindberg's [12] corresponding result for an elastic-plastic cylindrical shell with the same material and geometrical parameters. As mentioned above, these differences could be attributed to differences in definition as much as to differences in geometry. It does not appear possible to obtain simple expressions for the threshold velocities for cylindrical and spherical shells which have a common precise definition due to the different forms of the theoretical solutions. However, it would be worthwhile to generate amplification-impulsive velocity curves, such as those presented in Figs. 3 and 4, for both cylindrical and spherical shells with the same geometrical and material parameters. A comparison between these numerical results would then indicate whether spherical shells were indeed stronger than cylindrical shells as suggested by the expressions for the critical velocities.

The growth of the displacement and velocity amplification functions with time for typical elastic and elastic-plastic spherical shells are shown in Figs. 2 and 5, respectively. It is evident from these figures and Fig. 2 in Ref. [1] for the rigid-plastic case that the displacement functions experience larger amplifications than the velocity functions. This suggests that shape imperfections might exercise a more significant influence on the instability of spherical shells than variations in the initial velocity field.

It should be remarked that the constitutive equations do not cater for the influence of material strain-rate sensitivity which has been examined for cylindrical shells by Florence [13]. In addition to the various simplifications and approximations which are introduced in the theoretical analyses, the influence of transverse shear stresses and deformations have been disregarded. Moreover, the influence of unloading has been neglected so that the effect of possible plastic behavior after  $\tau = \tau_f$  has not been considered.

Finally, it should be remarked that only three terms have been retained in the series expansion (26c) which was used in the solution of an elastic-plastic spherical shell. The retention of more terms in this series would present complications but an examination of the importance of these additional terms might be one of many aspects worthy of further study.

†  $\bar{W}_y$  is the dominant transverse deflection at the onset of plastic flow when the additional strains due to the perturbed terms are neglected.

## CONCLUSIONS

A theoretical investigation has been undertaken into the dynamic instability of complete spherical shells loaded impulsively. If the various inequalities in the text are satisfied, then the elastic theory could be used to obtain the response of shells with large  $R/h$  ratios (e.g.  $R/h > 350$ ), while shells with small  $R/h$  ratios (e.g.  $10 < R/h < 60$ ) could be examined with the rigid-plastic theory which was presented in Ref. [1]. The elastic-plastic theory could be used to study those shells with intermediate values of  $R/h$ . Unfortunately, no experimental results are available to examine the validity, or otherwise, of the various theoretical predictions. However, the forms of the expressions for the critical mode number and threshold velocity are similar to those developed by various authors for cylindrical shells, except that the magnitudes of the numerical coefficients are different. The threshold velocities for the elastic, elastic-plastic and rigid-plastic spherical shells are larger than the corresponding values which have been published previously for cylindrical shells with the same  $R/h$  ratios and material parameters. The rigid-plastic theory presented in Ref. [1] predicts critical mode numbers for spherical shells which are somewhat similar to the corresponding experimental values on cylindrical shells with  $10 < R/h < 30$  which were reported in Refs.[14-16].

## COMMENTS ADDED AFTER REVIEW

The authors wish to thank a reviewer of this article for pointing out McIvor and Sonstegard's [17] article which had escaped our attention. McIvor and Sonstegard used a different procedure to examine the axisymmetric response of a linear elastic closed spherical shell which was subjected to a nearly uniform radial impulse. McIvor and Sonstegard show that the initial elastic response is governed by a Mathieu equation.† Thus, the amplitude of a member (or members) in the displacement series grow exponentially with time when the associated parameters lie within an unstable region of the Mathieu stability diagram. However, no information was obtained concerning the amplitude-wave number or amplitude-impulsive velocity relations as such shown for the linear elastic case in Figs. 2 and 3 of the present article. Clearly, threshold impulses cannot be determined without these results.

McIvor and Sonstegard then examined the long term elastic behavior for which it was necessary to retain additional terms in the governing equations. An approximate set of coupled equations was solved numerically for  $R/h = 100$  and  $V_0/C = 4.95 \times 10^{-3}$ .‡ These numerical results show that an essentially complete cyclic energy exchange occurs between the dominant mode and certain parametrically excited composite (membrane and bending) modes. This aspect of behavior was not investigated in the present article because the principal aim was to study dynamic instability which occurred prior to unloading.

It turns out that the elastic solution presented herein is not valid for the particular case considered by McIvor and Sonstegard because the inequality (34c) is not satisfied. Unfortunately, no other numerical results are presented in Ref. [17] so that a comparison cannot be made between the predictions of the two elastic methods. As intimated previously, it may be necessary to include additional terms in the series expansion (26c) in order to examine the elastic behavior of thicker shells than is presently permitted by the various inequalities. This appears to be a topic worthy for future study.

† See a previous footnote.

‡ This value is different to that quoted in Ref. [17] because McIvor and Sonstegard do not define  $C$  as given by equation (12d).



McIvor and Sonstegard [17] restricted their attention to both axisymmetric and linear elastic response. However, the importance of material plasticity can be demonstrated for the particular case examined in Ref. [17]. Equation (20a) with  $R/h = 100$ ,  $V_0/C = 4.95 \times 10^{-3}$  and  $\sin\sqrt{2}\tau = 1$  predicts  $\bar{W} = 0.35h$  when the elastic yield limit is reached (inequality (21) is an equality when  $\varepsilon_y = \sqrt{2}V_0/C = 7 \times 10^{-3}$ ). It is evident if imperfections are present that plastic flow would occur when the dominant transverse deflection is an even smaller fraction of the corresponding shell thickness.

*Acknowledgements*—The work reported herein was supported by the Structural Mechanics Branch of O.N.R. under contract number N00014-67-A-0204-0032. The authors wish to take this opportunity to express their appreciation to Mr. T. P. Boufounos for his assistance with the numerical computations.

#### REFERENCES

1. N. Jones and C. S. Ahn, Dynamic Buckling of Complete Rigid-Plastic Spherical Shells, A.S.M.E. paper 74-APM-W, *J. Appl. Mech.*, to be published.
2. R. M. Walters and N. Jones, An Approximate Theoretical Study of the Dynamic Plastic Behavior of Shells, *Int. J. Non-Linear Mech.* 7, 255-273 (1972).
3. N. Jones and C. S. Ahn, Dynamic Plastic Buckling of Complete Spherical Shells, M.I.T., Department of Ocean Engineering, *Report No. 73-19* (1973).
4. W. T. Koiter, The Non-Linear Buckling Problem of a Complete Spherical Shell Under Uniform External Pressure, *Proc. Kon. Ned. Akad. Wetenschappen* 72B, 40-123 (1969).
5. S. P. Timoshenko and J. M. Gere, *Theory of Elastic Stability*. McGraw-Hill (1961).
6. P. P. Bijlaard, Theory and Tests on the Plastic Stability of Plates and Shells, *J. Aero Sci.* 16, 529-541 (1949).
7. S. C. Batterman, Plastic Stability of Spherical Shells, *Proc. A.S.C.E.* 95, No. EM2, 433-446 (1969).
8. J. W. Hutchinson, On the Postbuckling Behavior of Imperfection-Sensitive Structures in the Plastic Range, *J. Appl. Mech.* 39, 155-162 (1972).
9. W. Stuijver, On the Buckling of Rings Subjected to Impulsive Pressures, *J. Appl. Mech.* 32, 511-518 (1965).
10. E. T. Whittaker and G. N. Watson, *A Course of Modern Analysis*. C.U.P. (1927).
11. H. E. Lindberg, Buckling of a Very Thin Cylindrical Shell Due to an Impulsive Pressure, *J. Appl. Mech.* 31, 267-272 (1964).
12. H. E. Lindberg, Dynamic Pulse Buckling of Cylindrical Shells, *Stanford Res. Inst. Tech. Rep.* 001-70 (1970).
13. A. L. Florence, Dynamic Buckling of Viscoplastic Cylindrical Shells, *Inelastic Behavior of Solids*, edited by Kanninen, Adler, Rosenfield and Jaffee, pp. 471-499. McGraw-Hill (1970).
14. G. R. Abrahamson and J. N. Goodier, Dynamic Plastic Flow Buckling of a Cylindrical Shell from Uniform Radial Impulse, *Proc. 4th U.S. Nat. Cong. Appl. Mech.* pp. 939-950 (1962).
15. H. Vaughan and A. L. Florence, Plastic Flow Buckling of Cylindrical Shells Due to Impulsive Loading, *J. Appl. Mech.* 37, 171-179 (1970).
16. W. C. Lyons, Elastic and Plastic Buckling of Cylindrical Shells Subjected to Impulsive Loads, *Arch. Mech. Stos.* 22, 111-123 (1970).
17. I. K. McIvor and D. A. Sonstegard, Axisymmetric Response of a Closed Spherical Shell to a Nearly Uniform Radial Impulse, *J. Acoust. Soc. Amer.* 40, 1540-1547 (1966).

**Абстракт** — Предпринимается теоретическое исследование вопроса динамической потери устойчивости полных сферических оболочек, внезапно нагруженных и изогнутых, либо из линейно упругого, либо из упруго-пластичного материала. Указывается, что некоторые гармоники быстро увеличиваются и являются причиной, для которой оболочки проявляют складчатую форму, изображенной числом критических форм выпучивания. Эти числа подобны для сферических и цилиндрических упругих оболочек, обладающих тоже самыми отношениями  $R/h$  и параметрами материала, но могут быть большими или меньшими для упруго-пластических сферических оболочек, в зависимости от значений разных параметров. Определяются, также, пороговые скорости, с целью получения самой меньшей скорости, которую оболочка может допускать без чрезмерной деформации. Пороговые скорости для упругих и упруго-пластических сферических оболочек больше по сравнению с такими же, которые были опубликованы раньше для цилиндрических оболочек, имеющих тоже самые отношения  $R/h$  и параметры материала.

## APPENDIX

*Constitutive equations for an elastic-plastic material*

The constitutive equations for an arbitrarily shaped shell which is made from an elastic-plastic material are developed in Ref.[3]. This Appendix contains a brief discussion of the derivation of equations (4a)–(4f).

If  $E_t$  is the tangent modulus of the strain-hardening portion of the equivalent stress ( $\sigma_e$ ) vs equivalent strain ( $\epsilon_e$ ) curve for a material, then the Prandtl–Reuss constitutive equations can be written

$$\dot{\epsilon}_{ij}^p = \frac{3J_2(\lambda - 1)}{4J_2 E} S_{ij}, \text{ or}$$

$$\begin{pmatrix} \dot{\epsilon}_{11}^p \\ \dot{\epsilon}_{22}^p \\ \dot{\epsilon}_{12}^p \end{pmatrix} = \frac{(\lambda - 1)}{4E} \begin{pmatrix} \alpha_0^2 - \alpha_0 \beta_0 & \gamma_0 \alpha_0 \\ -\alpha_0 \beta_0 & \beta_0^2 - \gamma_0 \beta_0 \\ \frac{\alpha_0 \gamma_0}{2} - \frac{\beta_0 \gamma_0}{2} & \frac{\gamma_0^2}{2} \end{pmatrix} \begin{pmatrix} \dot{\sigma}_{11} \\ \dot{\sigma}_{22} \\ \dot{\sigma}_{12} \end{pmatrix}$$

for the particular case of plane stress, where  $J_2 = \sigma_e^2/3$ ,  $\sigma_e = F\sigma_{11}$ ,  $F = (1 - q + q^2 + 3r^2)^{1/2}$ ,  $q = \sigma_{22}/\sigma_{11}$ ,  $r = \sigma_{12}/\sigma_{11}$ ,  $\alpha_0 = (2 - q)/F$ ,  $\beta_0 = (1 - 2q)/F$  and  $\gamma_0 = 6r/F$ . If the shear stress in the plastic range is small then  $r \ll 1$  and  $\gamma \approx 0$ . In this circumstance, combining the plastic strain rates with the corresponding elastic strain rates from Hooke's law gives

$$\dot{\epsilon}_{11} = (C_1 \dot{\sigma}_{11} - C_{12} \dot{\sigma}_{22})/4E, \dot{\epsilon}_{22} = (C_2 \dot{\sigma}_{22} - C_{12} \dot{\sigma}_{11})/4E, \text{ and } \dot{\epsilon}_{12} + \dot{\epsilon}_{21} = 2(1 + \nu)\dot{\sigma}_{12}/E,$$

where

$$C_1 = 4 + (\lambda - 1)\alpha_0^2, C_2 = 4 + (\lambda - 1)\beta_0^2, C_{12} = 4\nu + (\lambda - 1)\alpha_0\beta_0, C_3 = \Delta/(2 + 2\nu),$$

$$\Delta = (C_1 C_2 - C_{12}^2)/4, \alpha_0 = (2 - q)(1 - q + q^2)^{-1/2}, \text{ and } \beta_0 = (1 - 2q)(1 - q + q^2)^{-1/2}.$$

These equations may be inverted to obtain the stress rates which are then integrated with respect to  $z$  across the wall thickness of a shell to give the membrane forces and bending moments in the form of equations (4a)–(4f) provided  $q$  and  $\lambda$  are independent of  $z$  and  $\dot{\epsilon}_{ij} = \dot{\epsilon}_{ij} + z\dot{\kappa}_{ij}$ .